Exciton Simulations of Optical Spectra of the FMO Complex from the Green Sulfur Bacterium *Chlorobium tepidum* at 6 K

Simone I. E. Vulto,*,† Michiel A. de Baat,† Robert J. W. Louwe,† Hjalmar P. Permentier,† Tatjana Neef,† Mette Miller,‡ Herbert van Amerongen,§ and Thijs J. Aartsma†

Biophysics Department, Huygens Laboratory, Leiden University, P.O. Box 9504, 2300 RA Leiden, The Netherlands; Institute of Biochemistry, Odense University, Campusvej 55, DK-5230 Odense M, Denmark; and Biophysics Department, Free University, De Boelelaan 1081, 1081 HV Amsterdam, The Netherlands

Received: May 4, 1998; In Final Form: July 13, 1998

Optical spectra (absorption, circular dichroism, linear dichroism, and triplet-minus-singlet), measured at 6 K, are presented for the Fenna−Matthews−Olson (FMO) complex from the green sulfur bacterium *Chlorobium (C.) tepidum*. Significant differences are observed in comparison with the corresponding spectra of *Prosthecochloris (P.) aestuarii*. The spectra of *C. tepidum* FMO were simulated using exciton calculations, based on the recently resolved structure of this complex [Li et al. *J. Mol. Biol*. **1997**, *271* 456]. These calculations apply the same basic assumptions as were earlier used for the FMO complex from *P. aestuarii* [Louwe et al. *J. Phys. Chem. B* **1997**, *101*, 11280], except that the site energies of all but one of the bacteriochlorophylls had to be changed in order to optimize the simulations. The good agreement that was obtained supports the assumptions in these model calculations, and the assignment of the site energies makes it possible to consider the spectra in relation to the structural differences between the two types of FMO complex.

Introduction

The Fenna−Matthew−Olson (FMO) complex of *Prosthecochloris (P.) aestuarii* was the first pigment−protein complex, the structure for which was solved by X-ray crystallography.[1,2] It consists of an arrangement of three identical subunits, with a 3-fold rotational symmetry axis. Each subunit contains seven bacteriochlorophylls *a* (BChls), which gives a total of 21 pigments for the entire complex. The nearest-neighbor distances (center-to-center) within one subunit vary from 11.3 to 14.4 Å, while the distance between nearest neighbors in different subunits of the trimer is about 24 Å. Based on the well-defined structure, this system provides a critical test for the effect of exciton interactions on the electronic structure of the optically excited states and on the optical spectra. Although this complex has been characterized very well spectroscopically, simulations of the spectral properties were not very successful until recently.

The first simulations, in particular of the absorption and circular dichroism (CD) spectra, were performed by Pearlstein and Hemenger[3] using exciton calculations. After extensive simulations it was concluded that the spectra are determined not only by the dipolar coupling between the BChls, leading to excitonic shifts, but also by the fact that the BChls have different site energies due to different protein environments.[4−7]

A somewhat different approach was used by Gülen.[8] The CD spectrum, more than the other spectra, is very sensitive to the exact value and orientation of the transition dipole moments. Therefore, Gülen based her simulations on absorption, linear dichroism (LD), and triplet-minus-singlet spectra (T−S), using a fixed line width for all the optical transitions. However, when the same parameters were used to fit the CD spectrum, the results were not very satisfactory.[8]

Very recently, Louwe et al.[9] succeeded in simulating all the relevant optical spectra, absorption, LD, CD, T−S, and LD-(T−S), with a single set of parameters. The essential difference with the approach by Pearlstein and co-workers[6,7] and by Gülen[8] was the assumption of much smaller interaction energies between the BChl molecules, deduced in particular from inspection of the LD-(T−S) spectrum.[10] The simulations required an effective dipole strength of 28.7 D^2 of the BChls in FMO. Furthermore, only a single subunit was considered in the model calculations, since the relatively small effective dipole strength, together with the effect of disorder, also implied that interactions between pigments in different subunits are not significant. The parameter set was further minimized by assuming the same inhomogeneous line width for all optical transitions. A judicial choice of the site energies was based on the specific features of the LD, T−S, and LD-(T−S) spectra.[10] It was concluded that the structures of the spectra are dominated by variations in site energy, but nevertheless a significant exciton delocalization was obtained. The best simulation of the spectra was obtained when BChl 3, according to the numbering of Fenna and Matthews,[1] was assumed to have the lowest site energy.

Li et al.[11] recently solved the structure of the FMO complex of another green sulfur bacterium, *Chlorobium* (*C.) tepidum*, by X-ray crystallography. Only minor differences were found in the positions and orientations of the various BChls as compared to the case of *P. aestuarii*. However, the amino acid sequences show only 78% homology,[12] and the low-temperature absorption and CD spectra show significant differences. This indicates that the local environment and the site energies of the individual BChls in the FMO complex of *C. tepidum* will differ considerably from the corresponding ones in *P. aestuarii.*

* Corresponding author: e-mail vulto@biophys.leidenuniv.nl, fax 31-71-5275819.
† Leiden University.
‡ Odense University.
§ Free University.

10.1021/jp982095l CCC: $15.00
Published on Web 11/03/1998

In this paper we have applied exciton simulations to the optical spectra of the FMO complex from *C. tepidum*, with the site energies as adjustable parameters. The assignment of the various bands in the spectrum can then be used to relate the structural differences between *C. tepidum* and *P. aestuarii* to the observed spectroscopic differences. In the simulations, we considered a single subunit only and used the same value of the effective BChl *a* dipole strength as Louwe et al.[9] The same basic assumptions as used for FMO from *P. aestuarii* were taken as a starting point for the simulation of the optical spectra of *C. tepidum*. By changing the site energies of the various BChls as suggested by the spectroscopic data for *C. tepidum*, we achieved a good simulation for the absorption, CD, LD, and T−S spectra. A comparison is made between the simulation for FMO complexes from *C. tepidum* and *P. aestuarii*, and we have tried to relate the differences in electronic structure to the structural differences.

Materials and Methods

The FMO complexes of *C. tepidum* and *P. aestuarii* were purified according to the procedure described by Francke and Amesz.[13] The purity of the preparation was established by SDS-PAGE. The ratios of the peaks in the room-temperature absorption spectra are identical to those described by Olson et al.[14] and Miller et al.[15]

Low-temperature absorption spectroscopy was performed using a single-beam spectrophotometer as described elsewhere.[16] The spectral resolution was 1 nm. To obtain clear samples at low-temperature, glycerol (66% v/v) was added. Orientation of the FMO complexes was achieved by biaxial pressing[17,18] in a gel containing 8% acrylamide (w/v) and 55% (v/v) glycerol, stretching the gel by a factor of 1.6. The LD spectrum was measured as the difference in absorption of light with parallel and perpendicular polarization relative to the direction of stretching. The time-resolved triplet-minus-singlet (T−S) spectrum was measured with a single-beam spectrometer as described by Franken et al.[19] At room temperature, the sample had an absorbance of 0.4 at 809 nm.

The atomic coordinates of the FMO complex of *C. tepidum*[11] were kindly provided by Dr. J. P. Allen (Tempe, AZ). For exciton calculations, the dipole−dipole interaction between the various BChls was calculated in the point-dipole approximation.[9] The Q_y dipole moments of the individual BChls were assumed to be oriented parallel to the axis running trough the N_I-N_{III} nitrogen atoms. (Note that these are the N_B-N_D nitrogen atoms according to the crystallographic nomenclature.)

Results and Discussion

Experimental Spectra. Figure 1 compares the 6 K optical spectra of the FMO complexes from *C. tepidum* and *P. aestuarii*. The absorption spectra are shown in Figure 1A and are similar to the ones reported by Francke and Amesz.[13] The Q_y region of *C. tepidum* consists of at least four bands, centered at 795, 806, 815, and 825 nm. The 806 nm band has the highest amplitude. This is also observed in spectra of FMO from *C. limicola* f. *thiosulfatophilum*[20] and *C. phaeovibrioides*,[13] which are very similar. The FMO complex from *P. aestuarii* shows bands at 795, 800, 806, 814, and 825 nm. For this species, as well as for *C. vibrioforme*,[13] the band at 814 nm has the highest amplitude.

The CD spectrum at 6 K (Figure 1B) shows positive bands at 803 and 816 nm and negative bands at 790, 810, and 826 nm. It resembles the 77 K CD spectrum of *C. limicola* f. *thiosulfatophilum*,[21] as could be already expected on basis of the similarity of the absorption spectra and the 97% homology in amino acid sequences.[22] Significant differences are observed with the CD spectrum of FMO of *P. aestuarii* (Figure 1B). The latter shows positive bands at 801, 810, and 814 nm and negative bands at 790, 818, and 826 nm.

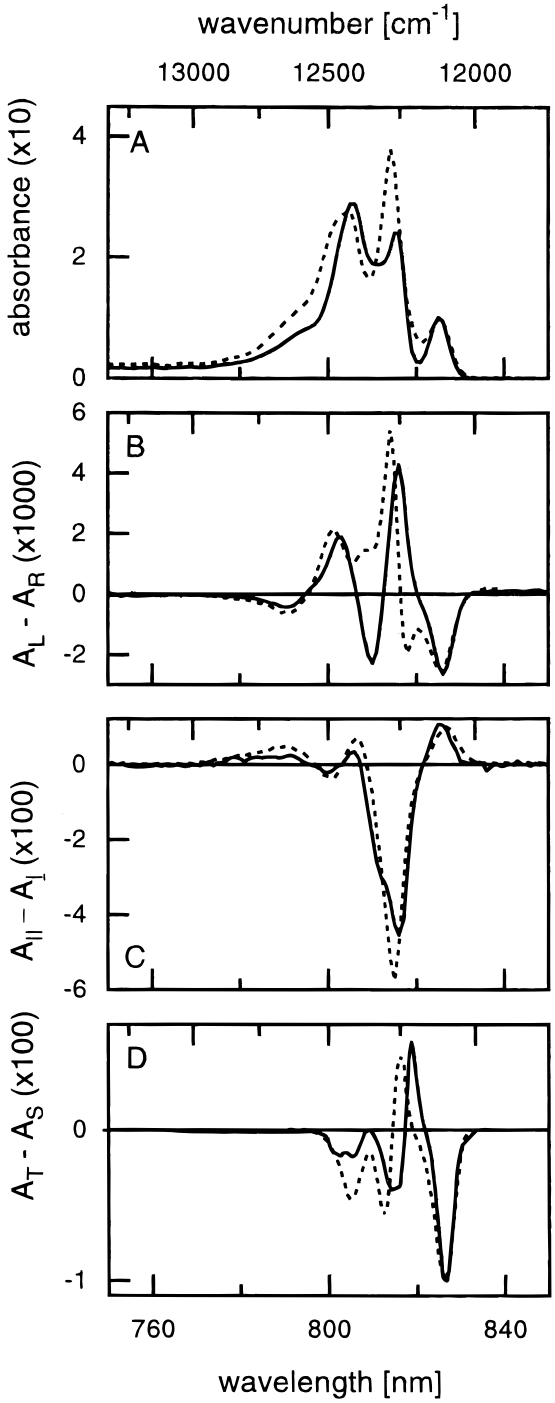

Figure 1. Optical spectra of the FMO complexes of *C. tepidum* (solid lines) and *P. aestuarii* (dashed lines) at 6 K: (A) absorption spectrum, (B) CD spectrum, (C) LD spectrum, and (D) T−S spectrum. The vertical scales refer to *C. tepidum*; the spectra of *P. aestuarii* were scaled to the same amplitude at 825 nm with respect to those of *C. tepidum*.

LD spectra are shown in Figure 1C. The spectrum of *C. tepidum* shows a large negative peak centered at 816 nm and minor bands at 800 and 812 nm (shoulder). Positive signals are observed at 806 and 825 nm, together with a broad positive band around 790 nm. It thus appears that the 825 nm band is

oriented at a large angle with respect to the 812 and 816 nm bands. This is in agreement with time-resolved anisotropy measurements of Savikhin et al.[23] Since FMO complexes are disklike particles, our orientation technique produces negative LD signals for transitions oriented more or less perpendicular to the plane of the trimer, whereas transitions that lie in the plane of the trimer give rise to a positive LD signal.[18] Accordingly, the negative band at 816 nm will correspond to one or more transitions that are roughly parallel and the positive bands to transitions approximately perpendicular to the C_3 axis. Inspection of the structure of FMO from *C. tepidum* shows that the transition moments of three molecules (BChls 1, 4, and 7) are oriented more or less parallel to the C_3 axis and those of the remaining BChls (BChls 2, 3, 5, and 6) roughly perpendicular to this axis.[11] This suggests, for example, a strong contribution of BChls 1, 4, or 7, or a combination of these, to the 815 nm band while the 825 nm band is expected to have a major contribution from one or more of the BChls 2, 3, 5, and 6. Except for the band at 812 nm, the LD spectrum of FMO complexes of *C. tepidum* is rather similar to the LD spectrum of FMO of *P. aestuarii* (Figure 1C and ref 24).

T−S spectra at 6 K are shown in Figure 1D. For each FMO complex the time constant for the decay was independent of wavelength. It was 70 μs for *C. tepidum* and 55 μs for *P. aestuarii*. The latter number is in agreement with that reported earlier.[24] The spectra show maximal bleachings at 827 nm, shifted to the red by 2 nm from the maxima of the corresponding bands in the absorption spectra. At shorter wavelengths we see an induced absorption at 819 nm and bleachings at 802, 805, and 814 nm in the *C. tepidum* spectrum. The relatively sharp features around 815 nm suggest a shift of the 815 nm absorption band upon triplet formation. Since the position of the main bleaching (827 nm) is the same and the shape of the T−S spectrum of *P. aestuarii*, with induced absorption at 816 nm and bleachings at 805, 813, and 827 nm, is similar to that of *C. tepidum*, it is likely that in both species the triplet carrying molecules are the same. The longer lifetime of the triplet state in *C. tepidum* might be related to the slight difference in planarity of the tetrapyrroles of the BChl 3 in both species.[25] The distance between the nitrogen atoms on the diagonal of the BChl *a* ring is 4.1 Å in *C. tepidum*, but 3.9 Å in *P. aestuarii*, suggesting that the Mg atom is more in the plane of the ring in *C. tepidum*.

Simulations. With respect to the relative orientations and distance of the BChls, the X-ray structures of the FMO complexes from *C. tepidum* and from *P. aestuarii* are very similar. This means that the differences in optical spectra must be ascribed to the differences in the protein structure. These then will give rise to differences of the local environment of the BChl *a* molecules and thus will affect the individual site energies. Therefore, the FMO complex of *C. tepidum* provides a critical test case for the basic approach that was used earlier in the successful simulation of the optical spectra of FMO from *P. aestuarii*.[9] The essential assumptions are (i) that only interactions within a single subunit are important, (ii) that all optical transitions have the same (inhomogeneous) line width of 80 cm^{-1}, (iii) that the effective dipole strength in calculating the interaction energies is equal to 28.7 D^2, and (iv) that hyperchromic effects are absent in the FMO complex. We have applied the same assumptions in simulating the optical spectra of FMO from *C. tepidum*. Simulations of the spectra of FMO from *P. aestuarii* showed that BChl 3 is the triplet carrying molecule. On the basis of the similarities in the T−S and LD spectra between both species, we used in our simulations the additional assumption that BChl 3 has the lowest site energy. For the 815 nm band we have restricted the candidates to BChls 1, 4, and 7, as concluded from the LD measurements (Figure 1C).

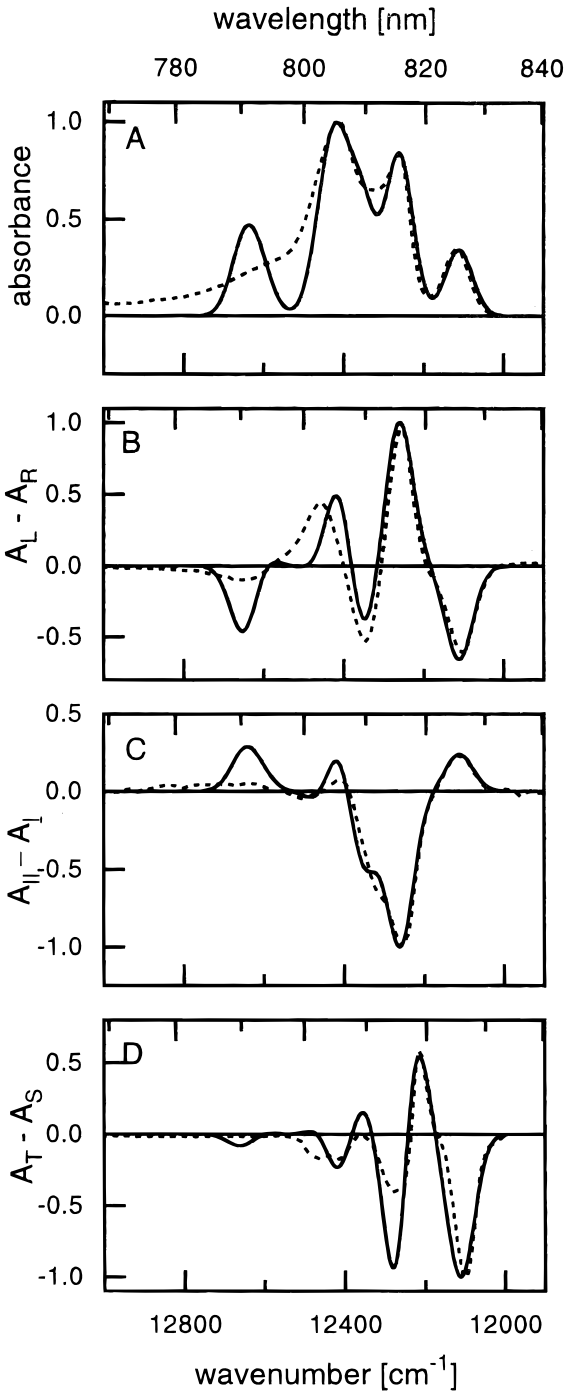

Figure 2. Simulations of the optical spectra at 6 K of the FMO complex of *C. tepidum* (solid lines): (A) absorption spectrum, (B) CD spectrum, (C) LD spectrum, and (D) T−S spectrum. The experimental values are plotted in arbitrary units as dashed lines. Parameters for the simulations are listed in Tables 1 and 2.

The results for the best simulation of the spectra of FMO complexes of *C. tepidum* are plotted in Figure 2. In Table 1 the corresponding site energies for the best simulations are given together with the dipole−dipole interactions between the various BChls as calculated from the structure. BChl 3 has the lowest site energy and BChl 2 the highest. The difference between the lowest and highest site energies is 460 cm^{-1}, comparable to the number for *P. aestuarii*[9] (440 cm^{-1}). The site energies

TABLE 1: Site Energies (Diagonal, Shown in Bold Italic) and Interaction Energies in Units of cm^{-1} Using BChl 3 as Triplet Carrying Molecule[a]

BChl no.	1	2	3	4	5	6	7
1	***12400***	**−106**	8	−5	6	−8	−4
2	**−106**	***12600***	**28**	6	2	13	1
3	8	**28**	***12140***	**−62**	−1	−9	17
4	−5	6	**−62**	***12280***	**−70**	−19	**−57**
5	6	2	−1	**−70**	***12500***	**94**	−2
6	−8	13	−9	−19	**94**	***12500***	**32**
7	−4	1	17	**−57**	−2	**32**	***12430***

[a] The largest dipolar couplings are given in bold.

for the individual BChls used in the simulation of the spectra of *P. aestuarii*, however, were significantly different.[9] The largest difference was found for BChl 2 (165 cm^{-1}); in most other BChls it was in the range 40−80 cm^{-1}. In contrast to *P. aestuarii*, the best fit was obtained with equal site energies for BChls 5 and 6. With respect to the dipole−dipole interactions, it may be noted that only nearest-neighbor interactions and the interaction between BChls 4 and 7 are important. The dipole−dipole interactions between the BChls are very similar to those in FMO of *P. aestuarii*,[9] which reflects again the strong resemblance between both structures and shows that the spectral differences can only be explained by differences in site energies. Diagonalizing the Hamiltonian results in the energies for the various exciton states and the corresponding eigenvectors as listed in Table 2.

Our results show that the degree of delocalization of excited state energies is relatively small. Only for the exciton states at 12 414 and 12 611 cm^{-1} is there a significant delocalization over more than one pigment, with nearly equal contributions of BChls 5 and 6, due to the identical site energies that had to be chosen for these two pigments (Table 1). An even larger dipolar coupling is found between BChls 1 and 2, but their site energies are quite different. Nevertheless, the two states at 12 355^{-} and 12 649 cm^{-1} contain a significant admixture of both BChl 1 and BChl 2.

Assigning a Gaussian band of 80 cm^{-1} to each transition results in the simulated absorption spectrum as shown in Figure 2A. The red part of the experimental absorption spectrum can be quite well reproduced, but some differences remain in the blue part of the spectrum. This is probably a result of the fixed (inhomogeneous) line width of 80 cm^{-1}, while based on the lifetime of the 790 nm band of ∼50 fs in both *C. tepidum*[26] and *P. aestuarii*[27] an additional homogeneous line width of ∼110 cm^{-1} should be taken into account. Furthermore, we have not included any vibrational bands or vibronic coupling effects, which are likely to contribute to the absorption in this region. Taking into account the lifetime broadening of the high-energy transition does significantly improve the simulation of the absorption spectrum. This can be achieved by convoluting the homogeneous line width, as measured by hole burning,[28] with a Gaussian inhomogeneous distribution function of 80 cm^{-1}, keeping all other parameters the same. This resulted mainly in a strongly reduced amplitude of the band at 12 650 cm^{-1} in all simulated spectra. However, to maintain the present focus of a first approximation, we prefer to show the optimal simulation in terms of the simplest model.

The simulated CD spectrum (Figure 2B) is in quite good agreement with the experimental data. When lifetime broadening for the highest-energy transitions is taken into account, all peaks in the simulations almost perfectly match the experimental spectrum (not shown). Since the CD spectrum is very sensitive to excitonic couplings, its simulation may be regarded as an important test for the description of the electronic structure of the FMO complex of *C. tepidum* and for the underlying assumptions.

The simulation of the LD spectrum is shown in Figure 2C. The red part can be well simulated. The shoulder at 812 nm is slightly more pronounced in the simulation than in the experimental data. This could be corrected by a shift of the site energy of BChl 1, but then the 815 nm band in the simulated absorption spectrum will become too high in amplitude.

The simulation for the T−S spectrum is plotted in Figure 2D. The main features can be quite well reproduced. The slight red shift of the 827 nm band in the experimental spectrum with respect to the simulation can be accounted for by slow energy transfer between the BChl 3 pigments in different subunits. Then the triplet state will be formed on the pigment with the lowest excited-state energy within the BChl 3 trimer.[10] This effect was not taken into account in the simulations.

If we now compare our results with the simulation for the FMO complex from *P. aestuarii* (Table 3), a few things can be noted at once. First of all, a different choice of site energies results in a reversed order of the states with largest contributions of BChls 1 and 4 when compared with the case of *P. aestuarii*. When we tried to make the situation more similar to *P. aestuarii*, the amplitude of the 815 nm band invariably became higher than the 806 nm band in the absorption spectrum. Conversely, when we interchanged the order of these site energies in *P. aestuarii*, the sign of the peak at 818 nm in the CD spectrum of *P. aestuarii* became positive. These results show that the shift of BChl 1 to higher energy in *C. tepidum* is responsible for the high amplitude of the 806 nm band in the absorption spectrum, the negative peak at 810 nm in the CD spectrum, and the shoulder at 812 nm in the LD spectrum. Second, as mentioned earlier, the site energies of BChls 5 and 6 were chosen equal for *C. tepidum*, which resulted in delocalization of the excited states at 12 414 and 12 611 cm^{-1} over BChls 5 and 6. Shifting BChl 5 to higher and BChl 6 to lower energy, like in *P. aestuarii*, deteriorated the simulated CD spectrum dramatically. Finally, the site energy of BChl 2 was shifted to

TABLE 2: Excited-State Energies (cm^{-1}), Dipole Strengths μ^2 (D^2), and Coefficients of the Eigenvectors Resulting from the Simulations Using the Parameters Plotted in Table 1[a]

		contribution of BChl no.						
excited-state energies	dipole strength	1	2	3	4	5	6	7
12 113	49.8	−0.04	−0.07	**0.92**	0.37	0.06	0.02	0.01
12 262	121.0	−0.06	−0.03	0.35	**−0.82**	0.28	0.10	−0.34
12 355	79.5	**0.91**	0.38	0.07	0.00	−0.10	0.09	−0.01
12 414	92.3	0.08	0.09	0.12	−0.33	**0.52**	**−0.73**	0.24
12 448	59.8	0.04	0.04	−0.08	0.18	0.39	−0.11	**−0.89**
12 611	27.6	0.09	−0.19	0.01	−0.22	**0.68**	**0.64**	0.17
12 649	52.2	−0.38	**0.90**	0.05	−0.02	0.11	0.18	0.04

[a] Contributions (c_{ij}) larger than 50% are shown in bold.

TABLE 3: Comparison between Simulations of FMO Complexes of *C. tepidum* and *P. aestuarii*; Results for *P. aestuarii* Are Taken from Ref 9[a]

C. tepidum			*P. aestuarii*		
excited-state energy	μ^2 (D^2)	BChl	excited-state energy	μ^2 (D^2)	BChl
12 113 (825.6)	49.8	3	12 112 (825.6)	46.7	3
12 262 (815.6)	121.0	4	12 266 (815.3)	151.5	1
12 355 (809.3)	79.5	1	12 293 (813.5)	57.2	4
12 414 (805.5)	92.3	5,6	12 396 (806.7)	89.3	6
12 448 (803.3)	59.8	7	12 457 (802.8)	90.7	7
12 611 (792.9)	27.6	5,6	12 496 (800.3)	11.7	2
12 649 (790.6)	52.2	2	12 634 (791.5)	35.5	5

[a] The excited-state energies are given in cm^{-1}; the numbers in parentheses are the corresponding wavelengths (nm). The numbers refer to those of the BChls contributing more than 50% to this exciton state (see Table 2).

much higher energy (165 cm^{-1}). It is known from literature that the transition energy of a chromophore can shift significantly, in some case more than 100 cm^{-1}, although the structure is identical (see for example the M210 mutant of reaction centers of *Rhodobacter sphaeroides*).[29,30] Therefore these differences must be due to variations in the local protein environment, the degree of hydrogen bonding, and the planarity of the porphyrin rings.

When the local environments of the BChls in the structures of both species are compared,[11] that of BChl 7 is most conserved, while significant differences are found for BChls 2 and 6. This is consistent with the site energies determined from the simulations of the spectra. Furthermore, the structure suggests that we can distinguish BChls 1 and 2, which are exposed on the surface of the monomer protein, from BChls 3−7, which are buried in the core of the subunit. Thus, it is conceivable that these BChls are less rigidly bound and hence are more susceptible to changes of the protein surroundings. Therefore, those BChls might show the largest differences in site energies. When the excited-state energy levels of both species are compared (Table 3), we note that here too the largest differences are found in the states which have the highest contribution of BChls 1 and 2 (12 355 and 12 649 cm^{-1} in *C. tepidum* and 12 266 and 12 496 cm^{-1} in *P. aestuarii*). Both states have shifted to higher energy *in C. tepidum* in comparison with *P. aestuarii*.

It may be assumed that the degree of hydrogen bonding has a significant effect on the site energies. From Raman spectroscopy of LH1 and LH2 complexes of several species of purple bacteria, Sturgis and Robert[31,32] concluded that the Q_y absorption maximum shifts toward lower energy when the degree of hydrogen bonding is enhanced. This can lead to a shift as large as 400 cm^{-1}, particularly when the C2 acetyl group is involved. Little information is available in the literature about a shift of the absorption maximum upon breaking the hydrogen bond to the C9 keto group. Hydrogen bonding may have a direct effect on the electronic wave functions, but it may also influence the absorption spectrum through changes in the local structure of the protein. When we compare the hydrogen bond lengths of the two FMO complexes, it seems that for all the BChls in the FMO complex of *C. tepidum* the hydrogen bonds are somewhat weaker than in *P. aestuarii*.[11] One hydrogen bond between a water molecule and the C9 keto group of BChl 5 in *P. aestuarii* has fully disappeared in *C. tepidum*, but remarkably, this is not correlated with a very large change in site energy. Furthermore, resonance Raman data indicate the presence of an additional C2 acetyl hydrogen bond in *P. aestuarii*, which is not present in *C. tepidum* (B. Robert, private communication). It is not clear at present which BChl is involved in this hydrogen bond.

Since the agreement between the simulated and the experimental CD spectra is significantly better for *C. tepidum* than for *P. aestuarii*,[9] we tried to improve the simulation for *P. aestuarii*. Louwe et al.[9] based their fit parameters for *P. aestuarii* on the LD, T−S and LD(T−S) spectra and calculated the CD spectrum afterward. Therefore, we now also included the fit of the CD spectrum as an important parameter for judging the quality of the simulations. However, the simulation of the CD spectrum (not shown) of *P. aestuarii* could only be improved at the expense of the other spectra. Therefore, we conclude that the simulation of Louwe et al.[9] still gives the best results.

Finally, we have also performed simulations on the whole trimer (not shown). This results only in minor improvements of the T−S spectrum, and the changes in other spectra are minimal, showing that the approach to use a single subunit only is correct. We have also considered the effect of disorder, in a similar way as Buck et al.,[33] but at the present level of approximation the effects are too small to be a significant improvement of the simulation.

Conclusions

We conclude that the assumptions for exciton simulations, as made by Louwe et al.,[9] like lowering the effective dipole strength and considering a single subunit only, give excellent results for the FMO complex of *C. tepidum*. By proper choice of the site energies, an even better simulation is obtained than for *P. aestuarii*. BChl 3 again is shown to be the lowest-energy pigment. Some of the spectroscopic differences between the FMO complexes of *C. tepidum* and *P. aestuarii* may be related to the structural differences in terms of hydrogen bonding and planarity of the porphyrin rings.

Acknowledgment. The authors thank Dr. C. Francke for the preparation of the FMO complex of *C. tepidum*. The atomic coordinates of the structure of the FMO complex of *C. tepidum* were kindly provided by Dr. J. P. Allen. Prof. J. P. Abrahams helped us with the interpretation of the crystallographic symmetry parameters. This work has been supported by the Life Science Foundation (SLW) and the Foundation for Chemical Research (SON), both financed by The Netherlands Organization for Scientific Research (NWO), and by the EC (Contract FMRX-CT96 0081). T. N. was supported by the Socrates Program for student exchange of the EC.

References and Notes

(1) Fenna, R. E.; Matthews, B. W. *Nature* **1975**, *258*, 573.

(2) Tronrud, D. E.; Schmid, M. F.; Matthews, B. W. *J. Mol. Biol.* **1986**, *188*, 443.

(3) Pearlstein, R. M.; Hemenger, R. P. *Proc. Natl. Acad. Sci. U.S.A.* **1978**, *75*, 4920.

(4) Pearlstein, R. M. In *Photosynthesis: Energy Conversion by Plants and Bacteria;* Govindjee, Ed.; Academic Press: New York, 1982; p 293.

(5) Pearlstein, R. M. In *Chlorophylls*; Scheer, H., Ed.; CRC Press: Boca Raton, FL, 1991; p 1047

(6) Pearlstein, R. M. *Photosynth. Res.* **1992**, *31*, 213.

(7) Lu, X.; Pearlstein, R. M. *Photochem. Photobiol.* **1993**, *57*, 86.

(8) Gülen, D. *J. Phys. Chem.* **1996**, *100*, 17683.

(9) Louwe, R. J. W.; Vrieze, J.; Hoff, A. J.; Aartsma, T. J. *J. Phys. Chem. B* **1997,** *101*, 11280.

(10) Louwe, R. J. W.; Vrieze, J.; Aartsma, T. J.; Hoff, A. J. *J. Phys. Chem. B* **1997,** *101*, 11273.

(11) Li, Y. F.; Zhou, W.; Blankenship, R. E.; Allen, J. P. *J. Mol. Biol.* **1997**, *271*, 456.

(12) Dracheva, S.; Williams, J. C.; Blankenship, R. E. In *Research in Photosynthesis*; Murata, N., Ed.; Kluwer Academic Publishers: Dordrecht, The Netherlands. 1992; p 53.

(13) Francke, C.; Amesz, J. *Photosynth. Res.* **1997**, *52*, 137.

(14) Olson, J. M. In *The Photosynthetic Bacteria*; Clayton, R. K., Sistrom, W. R., Eds.; Plenum Press: New York, 1978; p 161.

(15) Miller, M.; Cox, R. P.; Olson, J. M. *Photosynth. Res.* **1994**, *41*, 97.

(16) Francke, C.; Otte, S. C. M.; van der Heiden, J. C.; Amesz, J. *Biochim. Biophys. Acta* **1994**, *1186*, 75.

(17) Meiburg, R. F. Doctoral Thesis, Leiden University, The Netherlands, 1985.

(18) Abdourakhmanov, I. A.; Ganago, A. O.; Erokhin, Y. E.; Solov′ev, A. E.; Chugunov, V. A. *Biochim. Biophys. Acta* **1978**, *546*, 183.

(19) Franken, E. M.; Shkuropatov, A. Y.; Francke, C.; Neerken, S.; Gast, P.; Shuvalov, V. A.; Hoff, A. J.; Aartsma, T. J. *Biochim. Biophys. Acta* **1997,** *1321*, 1.

(20) Whitten, W. B.; Olson, J. M.; Pearlstein, R. M. *Biochim. Biophys. Acta* **1980,** *591*, 203.

(21) Olson, J. M.; Ke, B.; Thompson, K. H. *Biochim. Biophys. Acta* **1976**, *430*, 524.

(22) Hager-Braun, C.; Xie, D.; Jarosh, U.; Herold, E.; Buttner, M.; Zimmerman, R.; Deutzmann, R.; Hauska, G.; Nelson, N. *Biochemistry* **1995**, *34*, 9617.

(23) Savikhin, S.; Buck, D. R.; Struve, W. S. *Biophys. J.* **1997**, *73*, 2090.

(24) van Mourik, F.; Verwijst, R. R.; Mulder, J. M.; van Grondelle, R. *J. Phys. Chem.* **1994**, *98*, 10307.

(25) Gentemann, S.; Nelson, N. Y.; Jaquinod, L.; Nurco, D. J.; Leung, S. H.; Medforth, C. J.; Smith, K. M.; Fajer, J.; Holten, D. *J. Phys. Chem. B* **1997,** *101*, 1247.

(26) Buck, D. R.; Savikhin, S.; Struve, W. S. *Biophys. J.* **1997**, *72*, 24.

(27) Vulto, S. I. E.; Streltsov, A. M.; Aartsma, T. J. *J. Phys. Chem. B* **1997**, *101*, 4845.

(28) Franken, E. M.; Neerken, S.; Amesz, J.; Aartsma, T. J. *Biochemistry* **1998**, *37*, 7, 5046.

(29) Shochat, S.; Arlt, T.; Francke, C.; Gast, P.; van Noort, P. I.; Otte, S. C. M.; Schelvis, H. P. M.; Schmidt, S.; Vijgenboom, E.; Vrieze, J.; Zinth, W.; Hoff, A. J. *Photosynth. Res.* **1994**, *40*, 55.

(30) Shochat, S.; Gast, P.; Hoff, A. J.; Boender, G. J.; van Leeuwen, S.; van Liemt, W. B. S.; Vijgenboom, E.; Raap, J.; Lugtenburg, J.; de Groot, H. J. M. *Spectrochim. Acta A* **1995,** *51A*, 135.

(31) Sturgis, J. N.; Robert, B. *Photosynth. Res.* **1996**, *50*, 5.

(32) Sturgis, J. N.; Robert, B. *J. Phys. Chem. B* **1997**, *101*, 7227.

(33) Buck, D. R.; Savikhin, S.; Struve, W. S. *J. Phys. Chem. B* **1997**, *101*, 8395.